Gas Diffusion in Random-Fiber Substrates

A Monte Carlo (MC) technique involving explicit calculation of molecular trajectories in fibrous media is used to obtain effective transport coefficients in the Knudsen regime of gas diffusion. A fully penetrable cylinders (FPC) model is used to represent a fibrous substrate during the course of densification, as in composite fabrication processes such as chemical vapor infiltration (CVI). The calculated Knudsen permeabilities are in excellent agreement with available data. Accessible porosities are computed as a function of total porosity and are shown to depend on the fiber number density. The nonfiber phase is shown to percolate at $\phi \approx 0.095$, but the threshold is sensitive to the boundary conditions employed.

Rajesh R. Melkote
Klavs F. Jensen
Department of Chemical Engineering
and Materials Science
University of Minnesota
Minneapolis, MN 55455

Introduction

Chemical vapor infiltration (CVI) is a process used in composite manufacture which involves diffusion of gaseous reactants through a fibrous mat and subsequent deposition of solids on the fiber surfaces at elevated temperatures and low pressure (Kotlensky, 1973; Naslain et al., 1983). The process yields a fiber-reinforced composite of either carbon-carbon or two ceramic materials which can be used in high temperature applications requiring good oxidation resistance and high Young's moduli. Thus far, modeling of the gas transport through these fibrous substrates has largely ignored their structure and employed a tortuosity factor to estimate the effective diffusion coefficient (Rossignol et al., 1984). However, these substrates differ substantially enough from porous catalysts in their structure to merit study of the transport problem. Knowledge of the transport property evolution during the course of the infiltration is a crucial component of an overall model accounting for the diffusion and deposition phenomena. While porous catalysts are largely randomly disordered (with a few exceptions, e.g., zeolites), the deterministic solid phase geometry in the fibrous mats and substrates as seen in micrographs (Caputo and Lackey, 1984) offers some hope for including realistic features in a structural model.

The study of gas diffusion phenomena in porous materials, via both experiment and theory, has a rich history due to its immense importance in processes ranging from catalysis to membrane separations. The dependence of gas transport properties on the geometric details of the medium is generally complex and has been correlated empirically or through the use of network models. Fibrous media fall under a more general category of two-phase materials where one phase is distributed randomly as regularly shaped inclusions. The study of such materials can be traced to Maxwell (1881), who calculated the effective conductivity of a suspension of randomly distributed spheres in the dilute limit. Landauer (1952) used a cell approach (the precursor to modern-day effective medium theory) to obtain electrical conductivities in binary metal alloys with spherical inclusions. The convenient geometry of the latter has resulted in extensive analyses of porous materials comprised of randomly placed and possibly overlapping spheres. Rigorous bounds on diffusivity and permeability in random sphere media have been derived by Weissberg (1963), Strieder and Prager (1964), Weissberg and Prager (1970), and DeVera and Strieder (1977). In addition, several weighting or averaging techniques are available for the case of conductive inclusions (Kerner, 1956; Progelhof et al., 1976; McCullough, 1985). Conductivities of media comprised of arrays of cylinders have also been calculated (Keller, 1963; Guiffant and Flaud, 1986; Sangani and Yao, 1988). When randomness in orientation is introduced, usually Monte Carlo (MC) techniques are required (Ueda and Taya, 1985). A consequence of this randomness is the possibility of percolative behavior, that is, the abrupt appearance of a sample-spanning connected path at some critical volume fraction of inclusion. Percolation in 2-D and 3-D systems of conductive "sticks" was studied using MC by Pike and Seager (1974), Balberg and Binenbaum (1983), and Balberg et al. (1984). However, in the present case the cylinders (fibers) are insulating and their complement is the conducting phase. For this "inverse" case, considerably less information is available, due perhaps to the relative dearth of its application until the present interest in composite materials. Variational studies similar to those performed for spheres have established upper and lower bounds on

The present address of K. F. Jensen is Department of Chemical Engineering, Massachusetts Institute of Technology, Cambridge, MA 02139.

conductivities in media comprised of unidirectional and random fibers (Tsai and Strieder, 1986; Faley and Strieder, 1987, 1988), but there are no values for effective diffusivities for randomly oriented fibers.

While several capillary network models have been used for effective diffusivity calculations in porous media (e.g., Nicholson and Petropoulos, 1977), it is clear that in the case of fibrous substrates, any model which describes the diffusion as occurring through confined channels (as in cylindrical pores) is inadequate. An effective medium approximation (EMA) would require some knowledge of the bond distribution and nature of conductances; furthermore, EMA used alone has several limitations (Sahimi, 1988). Given the shortcomings of conventional techniques when applied to specialized materials, and concurrently with the growing sophistication of lattice calculations and computing resources, several works using explicit continuum models have appeared in recent literature (Evans et al., 1980; Abbasi et al., 1983; Smith, 1986; Burganos and Sotirchos, 1988). The first two papers have modeled the porous structure as assemblages of randomly placed solid spheres ("cannonball"), leading to pores with convex walls, and their "inverse," randomly punched spherical holes in a solid ("Swiss-cheese") which result in pores with concave walls and different critical behavior. Burganos and Sotirchos (1988) have accounted for pore overlap in explicit models of long cylindrical pores with randomly placed axes. Finally, in the case of CVI, a simplified model consisting of an array of intersecting cylinders with cubic symmetry has been used to calculate gas permeabilities in the preform (Starr, 1987).

The structure suggested here is one of fully penetrable cylinders (FPC) with randomly placed axes, which has been employed by Anderson (1986) as a model for surfactant structures and by Tsai and Strieder (1986), Torquato and Beasley (1986), and Faley and Strieder (1988) in studies of fibrous media. The latter have derived variational upper permeability bounds for 2-D and 3-D random fiber beds which are identical to the FPC construction. However, since the integral in their bound is dependent only on the void-solid geometry, their results are valid only for the Knudsen regime where the details of orientation and geometry govern the sequence of molecule-pore wall collisions. Moreover, the theoretical bounds, while useful, are roughly 40% higher than experimental permeabilities (Faley and Strieder, 1988). The FPC has no underlying network defined *a priori*. For the aforementioned "cannonball" model, Elam et al. (1984) tessellated the space into Voronoi polyhedra centered at the centers of spheres of equal radii, and found that the network formed by edges of the polyhedra in the void space captured the conductivity characteristics of the original model. The traditional MC methods could then be used to confirm scaling exponents for mean cluster size and correlation length, as well as the percolation threshold itself. However, Kerstein (1983) proved that if the "equal radii" restriction were to be removed, the same mapping could not be performed. In the present case, such a mapping, while highly desirable, does not appear likely. Thus, for complex but well characterized structures which are not amenable to the conventional network analyses, one must resort to explicit, albeit more computationally intensive, techniques. The latter include MC as well as solution of the diffusion equation in the void space subject to no-flux conditions at the inclusion surfaces using exact methods (Perrins et al., 1979), or multipol techniques (Sangani and Yao, 1988).

Theory

Structural model

The FPC model is meant to represent a 3-D section removed from a random assemblage of infinitely long right circular cylinders. A cylinder can be identified by the coordinates of a point on its axis (x_c, y_c, z_c), the direction cosines of the axis $(u_c, v_c, w_c$, of which only two are independent), and its radius, a total of six parameters. A cell of length L can be used as the simulation volume. Points are generated from a uniform distribution within the cell, and axis angles θ and Φ (see Figure 1) are generated from cosine and uniform distributions over $[0, \pi]$ and $[0, 2\pi]$, respectively. Finally, equal radii are assigned to all cylinders, although this restriction is not required.

The cylinders are allowed to overlap (and are thus penetrable to each other, but are obviously impermeable to diffusing molecules), which is a slight deviation from reality in the early stages of the CVI process. The reason for this allowance is two-fold. First, it is computationally much simpler to achieve structures of desired porosity if no attention is paid to possible overlap. An alternative procedure would be to generate the first cylinder, pick the second cylinder's axis and direction, and, if overlap is imminent, to "grow" the radius of the latter until it reaches the radius of the first one or just touches the first one, whichever occurs first. The procedure would be repeated with subsequent cylinders with an increasing number of checks being performed for steric conflicts. The resulting distribution of radii is not likely to be the desired one, and several iterations of this procedure will be required to achieve a specified radii distribution and porosity. A second alternative would be to generate the cylinders freely, but yet allow some bending in the fibers at points where intersection is imminent. While this realism can be implemented, its effect on gas transport is questionable.

Furthermore, at high porosities the degree of overlap in the FPC is negligible (see Figure 2), while as deposition of solids proceeds during CVI, interlocking of fibers occurs (cf., Figure 3

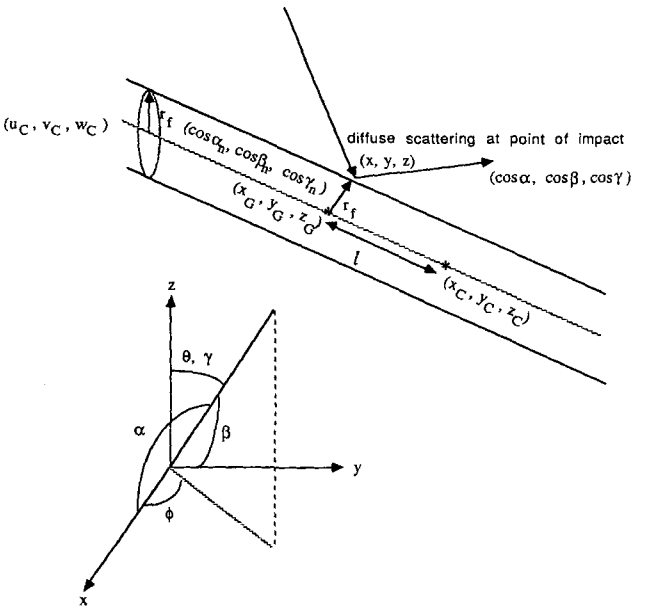

Figure 1. Cylinder-particle collision geometry; coordinate system.

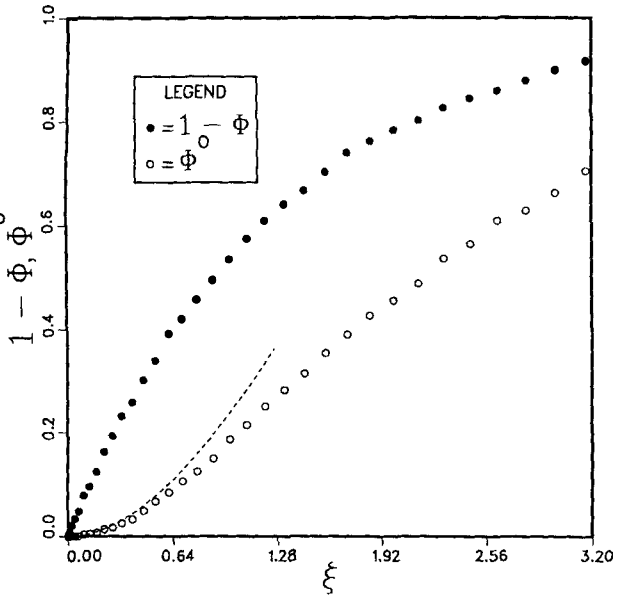

Figure 2. Overlap volume fraction vs. ξ.

in Caputo and Lackey, 1984) and the FPC again becomes a reasonable approximation at low porosities. Any error due to cylinder overlap is therefore greatest in the intermediate porosity range. Finally, cylinders generated in this manner will have their ends truncated where they intersect an edge of the cell. An average aspect ratio can be identified, which is only a function of the cell edge length and the manner in which the axis points were generated (Coleman, 1969). Typical average aspect ratios in our calculations were on the order of 20.

Characterization

The void fraction or porosity (ϕ) of the generated FPC structure is calculated using a rapid MC technique wherein points

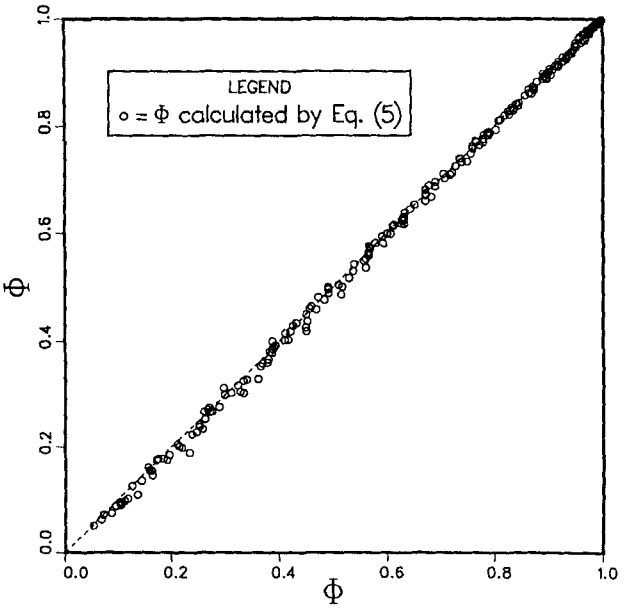

Figure 3. Accuracy of analytical expression for ϕ.

are chosen at random throughout the cell, and the fraction not occurring inside at least one cylinder is taken to be equal to ϕ. A sufficient number of points are chosen to reduce the error to ± 0.01; this typically requires on the order of 10^4 random points.

In estimating the mean pore dimension ($\bar{d}$) of such a structure, one has to confront the question of what constitutes a pore. In a void space that is the complement of an assemblage of solid cylinders, it is apparent that the pore walls will be convex. Foster (1986) has observed that for small aspect ratios, long (relative to the fiber radii) void passages of nearly constant cross section can develop in such a structure. In previous studies with similarly complex void spaces, two different interpretations of ($\bar{d}$) have been used. The more conventional one, used by Burganos and Sotirchos (1988),

$$\bar{d} = \frac{4\phi}{s} \tag{1}$$

where s is specific surface area, here given by (Anderson, 1986)

$$s = \frac{2\pi r_f \phi \sum_{i=1}^{N_c} l_{f_i}}{V} = -\frac{2}{r_f}\phi \ln \phi \tag{2}$$

Evans et al. (1980) take the average direct solid-to-solid distance covered by a molecule during a Knudsen regime simulation to approximate $\bar{d}$, and find a difference of only a few percent with $\bar{d}$ as estimated by a stereological technique involving the casting of random lines across the solid. A third related technique is suggested by Tokunaga (1985) who derived a density for Knudsen free paths, ℓ:

$$f(\ell) = 1/\bar{\ell}\, e^{-\ell/\bar{\ell}} \tag{3}$$

The solid-to-solid distances can be stored during the course of the simulation, and their distribution can be fitted to the form of Eq. 3, from which $\bar{\ell}$ can be retrieved. Here it was found that, over a wide range of porosities, the three methods (excluding the random lines method) yielded very similar numbers, with the Knudsen free path methods becoming less reliable at higher porosities. Therefore, the simpler Eq. 1 will be used exclusively (unless otherwise noted).

In making the connection between the model and the real system, one should note that ϕ and $\bar{d}$ will depend on the fiber radius (r_f) as well as on the number density of fibers (n_f). Gavalas (1980) showed that for uniformly sized cylindrical capillaries of radius r with axes whose intersections with a fixed plane are Poisson distributed,

$$1 - \phi = \exp\left[-2\lambda' \pi r^2\right] \tag{4}$$

where $\lambda' = \frac{1}{2}$ (total length of pore axes per unit volume). Since the FPC is essentially the "inverse" of Gavalas' construct, we have

$$\phi = \exp\left[-\pi r_f^2 \frac{\Sigma l_{f_i}}{V}\right] = \exp\left[-\pi r_f^2 n_f \bar{l}_f\right] \tag{5}$$

where $\bar{l}_f$ is the mean length of fibers. The relation (Eq. 5) holds down to very low porosities (Figure 3) and it implies $\bar{l}_f \to \infty$ as $\phi \to 0$. It is the analog of the well known result for random spheres (Weissberg, 1963),

$$\phi = \exp\left[\frac{-4}{3}\pi\rho r_s^3\right] \tag{6}$$

where ρ = number density of spheres. Figure 3 is a measure of how closely the simulation volume, with a finite number of cylinders, mimics the real infinite FPC system.

Equation 5 suggests a convenient dimensionless group for characterizing the fibrous structure. One can define

$$\xi \equiv \frac{d_f^2 \Sigma l_{f_i}}{V} = 4r_f^2 n_f \bar{l}_f \tag{7}$$

which implies that the total length of axes per volume is a key experimental quantity (confirming a similar observation by Ogston, 1958). Furthermore, combining Eqs. 1, 2, and 7, yields

$$\frac{\bar{d}}{r_f} = \frac{8}{\pi\xi} \tag{8}$$

The relationship (Eq. 8) suggests that the fiber radius determines the mean pore dimension given ξ, or, equivalently, that ξ alone is insufficient for describing the structure. Two structures with the same ξ can have different inter-fiber spacings and thus different Knudsen diffusivities, which are strongly dependent on $\bar{d}$. Caution should be exercised, however, in equating $\bar{d}$ to the mean pore diameter obtained by porosimetry measurements on fibrous substrates.

The dimensionless group, ξ, has been used in a similar context in a different physical problem, that of solute partitioning in fibrous membranes [Fanti and Glandt, in press]. If the fibers are represented by sticks having zero volume, and a solute molecule has diameter d,

$$\xi = \frac{d^2 \Sigma l_i}{V} \tag{9}$$

Here the inter-fiber spacing is equal to the diameter of the largest solute molecule that can "fit." There is not a one-to-one correspondence with the FPC structure because the penetrability and finite radii of the cylinders in the latter leads to a significant volume of overlap (ϕ^o) requiring a parameter quantifying $\bar{d}$. Figure 2 shows the overlap fraction, ϕ^o. For $\xi < 4/\pi$, the overlap can be calculated by the simple formula:

$$\phi^o = \frac{\pi}{4}\xi + e^{-(\pi/4)\xi} - 1 \tag{10}$$

which is shown as a dashed line in Figure 2. For $\xi > 4/\pi$, the fraction of overlap volume is a complex function of the particular configuration which must be evaluated numerically.

Since isotropy is a key feature of many short-fiber substrates typically used in CVI, the computer-generated structures were tested for homogeneity by calculating porosity and mean pore dimension over different sections of the cell, and checking that they differ by no more than a few percent, except for very low fiber densities, as might be expected. As a consequence, the Knudsen diffusion is isotropic, i.e.,

$$D_K = D_{K_x} = D_{K_y} = D_{K_z} \tag{11}$$

Knudsen regime

Simulation technique. The Knudsen molecular flux through a slab of length L is given by

$$\text{flux} = \frac{N_0 D_K^{\text{eff}}}{RT}\frac{\Delta p}{L} \tag{12}$$

where the model equation for the effective Knudsen diffusivity is based on kinetic theory (Abbasi et al., 1983; Burganos and Sotirchos, 1988):

$$D_{K_i} = \lim_{\Delta s_i \to \infty}\left(\frac{f_T \Delta s_i \bar{v}}{4}\right) \tag{13}$$

Here, f_T is the fraction of molecules transmitted to a distance greater than or equal to Δs_i in the direction of diffusion i, and $\bar{v}$ is the average thermal velocity of the molecules. This further implies that a plot of f_T vs. $1/\Delta s_i$ should yield the Knudsen diffusivity, D_{K_i}. This suggests an MC algorithm wherein a simulation volume elongated in one direction (such as the x-direction in Figure 4) can be used to collect (f_T, Δs_i) data. Specifically, test molecules can be initiated at the void portions of the $x = 0$ face with initial cosines directing them into the cell, with subsequent trajectories taking them from solid surface to solid surface. For those molecules which traverse some distance into the cell and reemerge at $x = 0$, their maximum x-penetration depths are stored. Among the rest, some will emerge at $x = L$ and the remainder will be "trapped," that is, will not emerge from either edge after some maximum number of steps. The latter fraction is allowed to take this maximum number of steps and then their maximum penetration depths are recorded.

Details. Consider a single "test molecule" described above. It is given an initial coordinate, $x = 0$, and various y- and z-coordi-

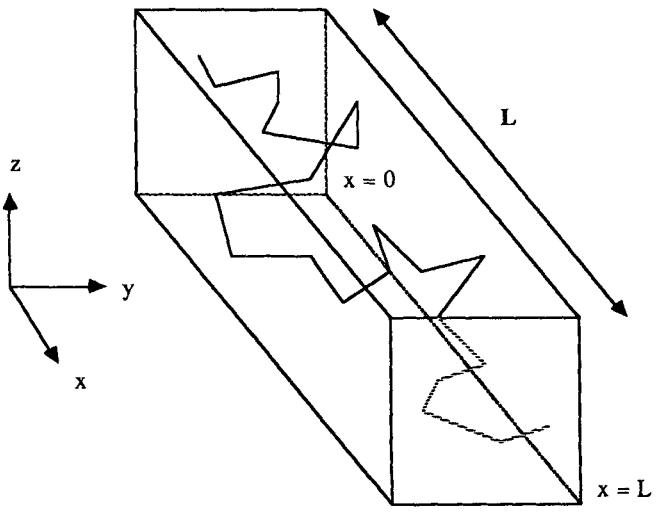

Figure 4. Typical molecular trajectory in simulation volume.

nates are tested until a point $(0, y, z)$ is found to be in the void space. The molecule is then given an x-direction cosine > 0, and a y-direction cosine at random so that the first step carries it into the cell. Using these cosines, a search is performed over all cylinders to determine the one closest to the current point. In order for the cell boundaries to be conveniently included in the search, they are represented by cylinders of very large radii which are tangent to the six cell edges (Abbasi et al., 1983). The search consists of compiling a list of distances to all cylinders whose outer surfaces intersect the trajectory line. If the search dictates a collision with an internal cylinder, the molecule is advanced accordingly and new direction cosines ($\cos\alpha$, $\cos\beta$, $\cos\gamma$) are calculated using θ and Φ as follows:

$$\Phi \text{ uniform} \in [0, 2\pi]$$

$$\theta \sin \in \left[-\frac{\pi}{2}, \frac{\pi}{2}\right]$$

The new cosines are computed using the direction cosines of the normal to the current cylinder surface, so that a trajectory is not generated which leads to penetration of the solid phase:

$$\cos\alpha = \cos\alpha_n \cos\theta + \sin\alpha_n \sin\theta \cos\Phi$$

$$\cos\beta = \cos\beta_n \cos\theta + \sin\beta_n \sin\theta \cos a$$

$$a = \frac{\pi}{2} + (\text{sgn}\cos\alpha_n)\left(\frac{\pi}{2} - \Phi\right) + (\text{sgn}\cos\gamma_n)\cos^{-1}\left(\frac{\tan\left|\frac{\pi}{2} - \alpha_n\right|}{\tan\beta_n}\right)$$

$$\cos\gamma = \pm(1 - \cos^2\alpha - \cos^2\beta)^{1/2} \qquad (14)$$

The sign on $\cos\gamma$ is chosen so as to satisfy the geometric constraint

$$\cos\alpha\cos\alpha_n + \cos\beta\cos\beta_n + \cos\gamma\cos\gamma_n = \cos\theta \qquad (15)$$

and the direction cosines of the normal to the cylinder surface at the point of impact (x, y, z) are (see Figure 1)

$$\cos\alpha_n = \frac{(x - x_g)}{r_f}; \quad \cos\beta_n = \frac{(y - y_g)}{r_f}; \quad \cos\gamma_n = \frac{(z - z_g)}{r_f}$$

$$x_g = x_c + u_c t$$

$$y_g = y_c + v_c t$$

$$z_g = z_c + w_c t$$

$$t = \pm((x - x_c)^2 + (y - y_c)^2 + (z - z_c)^2 - r_f^2)^{1/2} \qquad (16)$$

Here, the sign on t is determined by whether the + or − results in cosines which satisfy

$$\cos^2\alpha_n + \cos^2\beta_n + \cos^2\gamma_n = 1 \qquad (17)$$

If however, the search indicates that a collision with a y- or z-boundary cylinder (transverse to the direction of diffusion) is imminent, the molecule is displaced away from that boundary by a distance equal to the y- or z-dimension of the cell, as shown in Figure 5. The cosines are preserved, and the search is repeated. The molecule is then sent to the closest cylinder such that its intersection with the trajectory is within the cell boundaries. This procedure is the application of "fully periodic" boundary conditions. In the past MC work (Evans et al., 1980; Burganos and Sotirchos, 1988), specular reflection has been used at the boundaries to extend the sample to infinity in the transverse directions. If applied here, the fibers are effectively bent at the cell edges. This not only introduces an artificial symmetry into the problem but has serious implications for the calculation of isolated porosity, as will be shown in a later section. A quantity of interest readily generated during the course of the trajectory is the distribution of Knudsen free paths, an example of which is shown in Figure 6. It is seen to qualitatively follow the exponential form suggested by Eq. 3.

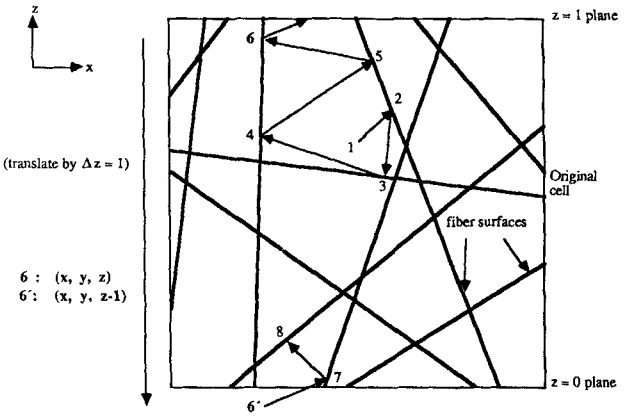

Figure 5. Toroidal boundary condition.

The fraction transmitted data generated in this manner is biased by the fact that all test molecules originate in the void. Assuming that void area fraction is roughly equal to void volume

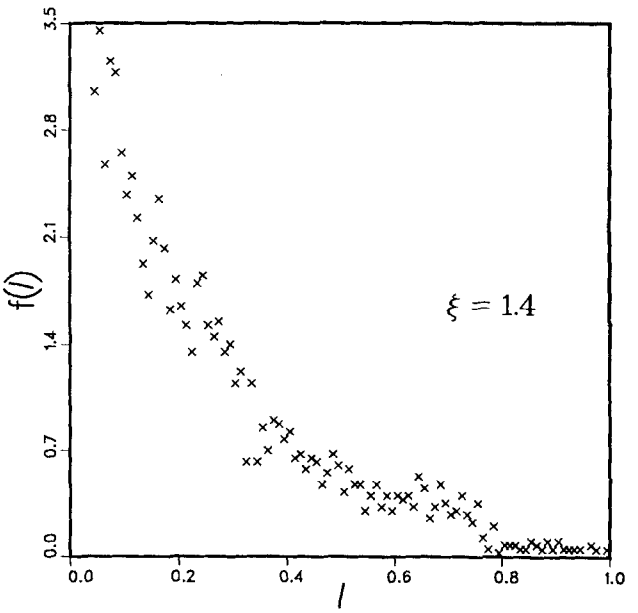

Figure 6. Knudsen free path distribution.

fraction, on the average, $f_T = \phi f'_T$ (where f'_T is obtained from the simulation) will be the true fraction transmitted. The slope obtained from the plot must be multiplied by ϕ to compensate for this bias (see Eq. 22).

Statistical issues. The first issue of interest involves how large L should be. Note that ideally a plot of f'_T vs. $1/\Delta s_i$ should go through the origin ($f'_T \to 0$ as $1/\Delta s_i \to \infty$). Starting with $L = 1$ (unit cell), f'_T vs. $1/\Delta s_i$ data were compiled for a particular n_f and plotted, but when extrapolated the line did not pass through the origin. It was deemed necessary to increase to $L = 3$ until this occurred. In the simulations thereafter, this value of L was retained. Second, an adequate number of test molecules (n) must be used to compensate for end effects resulting from initiating all molecules at the $x = 0$ plane. This was accomplished by choosing n to have a base value of $n_0 = 2{,}500$ (based on literature), and then testing the significance of $\bar{D}_{n_j} > \bar{D}_{n_0}, j = 1, 2, \ldots$ against the null hypothesis, $\bar{D}_{n_j} = \bar{D}_{n_0}$. The choice of n_0 was dictated by the minimum number required to give a good linear fit for one trial, but never exceeded 3,500. Last, the number of trials (N_T) of n molecules was each determined such that the 95% confidence interval on $\bar{D}^{\text{eff}}/D(\bar{r})$ was lowered to $\pm 10\%$ or less; typically, 10–15 trials were required.

Accessible porosity

The quantity of interest, ϕ^A, represents the volume fraction that is void and accessible to transport across the sample. In the present case, ϕ^A is necessary in determining the effective transport coefficient in the ordinary regime (Reyes et al., 1988):

$$\frac{D^{\text{eff}}}{D^{\text{bulk}}} = \frac{\phi^A}{\tau} \tag{18}$$

as well as in determining the accessible specific surface area for reaction.

The MC algorithm for calculating ϕ^A as a function of ϕ and n_f is patterned after the Knudsen calculations. The difference is that test molecules are initiated in an internal void. The particle is then allowed to repeatedly strike solid surfaces (with diffuse scattering at each) until it strikes $x = 0$ or $x = L$. If this occurs, the molecule is specularly reflected back into the cell. Note that specular reflection can be used here since the finite cell is of interest. If, in less than $n_{\max}$ total steps, the particle also strikes the opposite x-face, it is tallied as having originated in an accessible ("open") part of the void space. However, in $n_{\max}$ steps it may hit only one or none of the x-faces, in which case the originating pore is designated "closed" (isolated or dead-end porosity). We approximate

$$\phi^A \approx \frac{(\text{number open})}{(\text{total number})}\,\phi \tag{19}$$

provided we take enough molecules. Again, fully periodic boundary conditions are applied in the y- and z-directions.

Statistical issues. The total number required to constitute a sufficient sample and avoid bias towards particular regions of the cell was determined by observing the behavior of ϕ^A vs. N_M; this is shown in Figure 7. It appears that for the cases illustrated, $N_M \geq 200$ produces a negligibly different result. This was

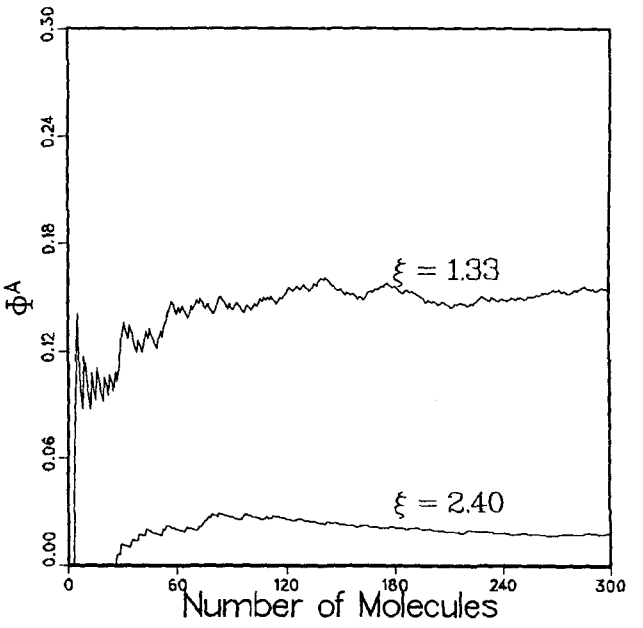

Figure 7. Calculation of ϕ^A.

repeated for a few other cases and $N_M = 300$ was used as a number which would be universally sufficient. Again, $L = 3$ was used, primarily to compare results with the Knudsen case. Fixing the value of $n_{\max}$ is nontrivial. Initially, $n_{\max} = 2{,}000$ was used. As this limit was increased, more particles "escaped" and ϕ^A shows an apparent increase. Ideally, one would want to tally as "closed" those molecules which would not emerge even if $n_{\max} = \infty$. However, since this is not a lattice model where a node has a certain fixed number of nearest neighbor bonds, and since the test molecules are point particles, "closed" or "inaccessible" are necessarily relative terms. For practicality, $n_{\max}$ was increased until the resultant ϕ^A differed negligibly; this was around $n_{\max} = 5{,}000$. This implies that increasing the sample size, L, is doubly expensive for computation: the number of cylinders has to be increased to maintain n_f (which adds time to the search procedure), and $n_{\max}$ must be increased as well. Finite size effects will be discussed further in the following section.

Discussion of Results

Knudsen diffusion

The Knudsen diffusivity obtained by the technique based on Eq. 13 is determined up to a factor of $\bar{v}$ and the length scale Δs_i by the relation

$$f'_T = \left(\frac{4D_{K_i}}{\bar{v}}\right)\frac{1}{\Delta s_i} = (\text{slope})\,\frac{1}{\Delta s_i} \tag{20}$$

where $\bar{v}$ for a Maxwell-Boltzmann density is given by

$$\bar{v} = \left(\frac{8RT}{\pi M}\right)^{1/2} \tag{21}$$

Therefore, to present the results in a general manner, D_K is normalized by $D_{K_0} = \frac{1}{3}\bar{v}d_0$, the Knudsen diffusivity in a hypotheti-

cal pore of diameter, d_0,

$$\epsilon \equiv \frac{D_K}{D_{K_0}} = \frac{3}{4}\phi\frac{(\text{slope})}{d_0} \tag{22}$$

In Figure 8, diffusivities for three fiber number densities (indicated by different symbols) as a function of ϕ are presented, normalized by $d_0 = \bar{d}$, as defined by Eq. 1. When this basis is used, the qualitative behavior of the ϵ vs. ϕ curves is very similar to the effective conductivity vs. ϕ curves for random 3-D tessellations such as cubic and Voronoi (Reyes, 1985). Since $\bar{d}$ is a function of ϕ and diverges as $\phi \rightarrow 1$, a choice of d_0 independent of ϕ would more naturally reveal the trend of D_K vs. ϕ. Figure 9 shows the same results as Figure 8 but now normalized by $d_0 = \bar{d}$ at $\phi = 0.50$. These curves all show a sharp rise in D_K at high ϕ, a trend consistent with the behavior in systems of parallel, overlapping cylindrical pores (Burganos and Sotirchos, 1988) and physical intuition, since D_K, being heavily dependent on geometry, should increase as the structure "opens up." A common feature appears to be the fact that D_K appears to go to zero at nonzero ϕ, suggesting the existence of a percolation threshold (ϕ_C) in the vicinity of $\phi \lesssim 0.1$. Figure 10 shows the results of Figure 8 plotted against the parameter, ξ. An interesting feature is that the data almost collapse to a universal curve; however, there is a slight variation with number density (and correspondingly, mean pore dimension) which might be expected. For the problem of solute partitioning in fibrous membranes, Glandt (1989) has conjectured that the percolation threshold occurs at a reduced matrix density, $\xi = 3$, which would correspond to $\phi = e^{-(3\pi/4)} = 0.095$. The data in Figure 10 seem to confirm this idea to within experimental error of the numerical scheme. This value can be compared to $\phi = 0.034$ for monodisperse spheres (Elam et al., 1984). Further evidence of a common threshold value will appear in the ϕ^A results. While each data point in Figures 8–10 represents a different generated structure, the error bars represent 95% confidence limits on averages over samples of N_M particles.

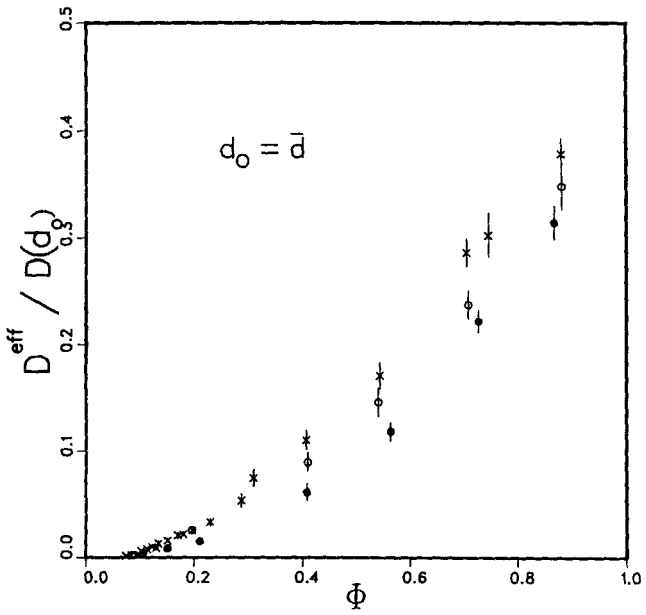

Figure 8. $D^{eff}/D(\bar{d})$ vs. ϕ.

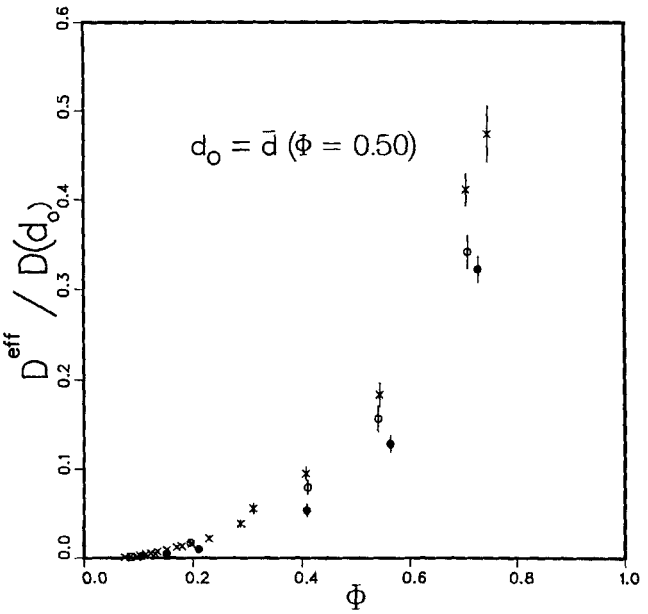

Figure 9. $D^{eff}/D(d_0)$ vs. ϕ.

Accessible porosity

ϕ^A was calculated using the "open"/"closed" classification technique described earlier. ϕ^A was computed as a function of ϕ for a few number densities, and the results are summarized in Figure 11. The features of note are that, first, ϕ^A appears to go to zero at $\phi \lesssim 0.10$, thus confirming what the Knudsen results suggest. Second, the value of ϕ at which ϕ^A begins to deviate from $\phi^A = \phi$ (dotted line in Figure 11) appears to increase with n_f. This is an intuitive result as well, since if n_f is higher, as r_f is increased there is a higher probability of forming a small isolated region (cluster) than at a lower density, for identical ϕ. Marinkovic' and Dimitrijevic' (1985) found experimentally that the open porosity during infiltration at the same apparent substrate density differed with fiber content, and similarly concluded that this was due to a higher probability for "pore clogging" when the average fiber spacing is smaller. The effect of n_f on the percolation threshold $\phi_C (\equiv \phi(\phi^A = 0))$ is difficult to determine from Figure 11 due to the increasing uncertainty as ϕ gets small. The latter uncertainty is due to finite size effects; ϕ_C is defined as the void fraction at which an infinite (sample-spanning) cluster first appears. Using a finite L necessarily introduces a limitation. However, ϕ_C can be estimated by various techniques (Sahimi, 1988). In Figure 12, the same data is plotted against the dimensionless group, ξ. Figure 12 suggests a threshold which is consistent with the value, $\xi = 3$ (Glandt, 1989), but not as strongly consistent as Figure 10, due to the greater amount of scatter in ϕ^A.

Figure 11 was generated by assuming fully periodic (or equivalently, toroidal) boundary conditions. All past MC simulations of gas diffusion, however, have used the specular reflection boundary condition, perhaps due to its ease of implementation (Nakano and Evans, 1983). Recently, Fanti and Glandt (1989) have simulated hard sphere fluids in fibrous media confined to the surface of a four-dimensional hypersphere. While this eliminates edge effects, it introduces curvature into the system, which requires taking a sufficiently large hypersphere. It appears to have the greatest advantage over conventional boundary condi-

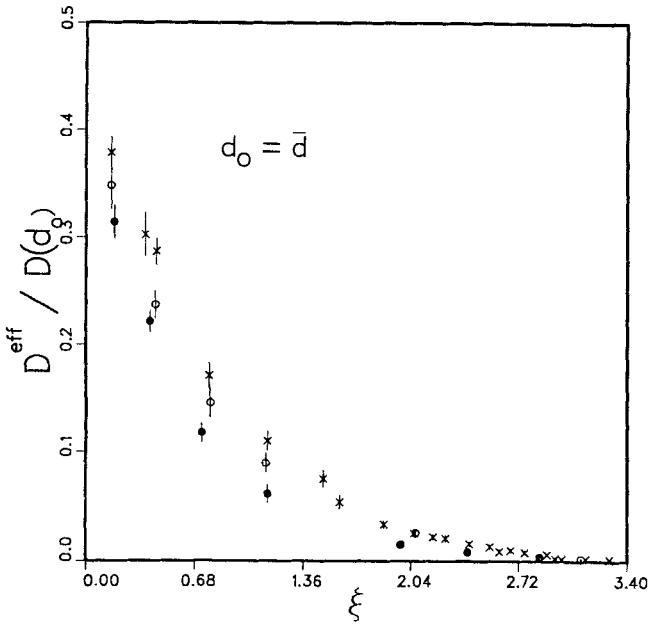

Figure 10. $D^{eff}/D(\bar{d})$ vs. ξ.

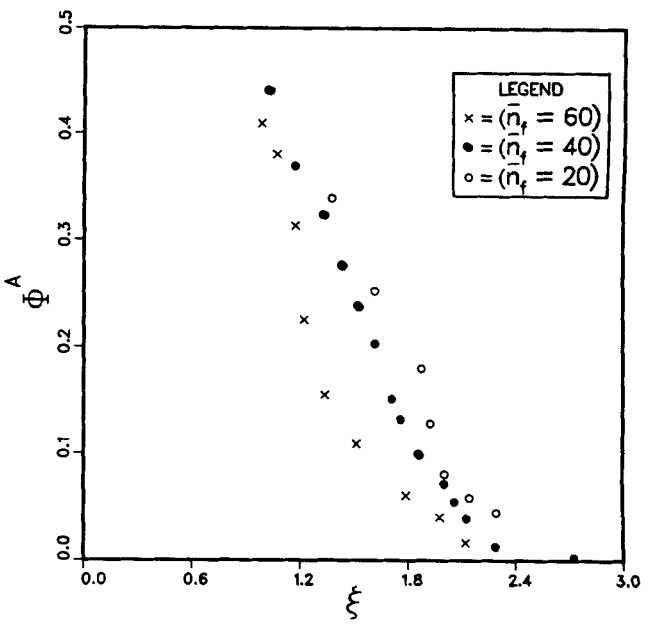

Figure 12. Accessible porosity vs. ξ.

tions when the inhomogeneities of the medium are of a scale larger than the characteristic length of the system (the cell size in this case). In the current study, the boundary conditions were found to seriously affect the calculation of accessibility characteristics of the medium. This is probably due to the formation of spurious clusters resulting from the specular condition. Specifically, if the configuration of the solid is as shown in Figure 13 where the edge of the cell and some adjoining cylinders form a small pocket, then application of the specular condition implies reflecting the solid around the edge. If a test molecule originates in the pocket or arrives there during the course of the simulation, it is quite conceivable that it could spend all of its time "bouncing" from cylinder to cylinder within that pocket. This would have the effect of exaggerating the closed fraction, by inadvertently forming pseudo-clusters. The ϕ^A vs. ϕ curves generated using the specular condition are shown as a function of n_f in Figure 14. It can be seen that the percolation threshold inferred from such a plot can be almost twice the more realistic value inferred from Figures 11 and 12. While the toroidal condition undoubtedly introduces some long-range correlations, it is an improvement over the specular condition. For densified fibrous media at the end of infiltration, several CVI studies have reported "residual porosities" of 0.05–0.15 (Pfeifer et al., 1970; Pierson, 1975; Colmet et al., 1986) which would support present results obtained with toroidal boundary conditions.

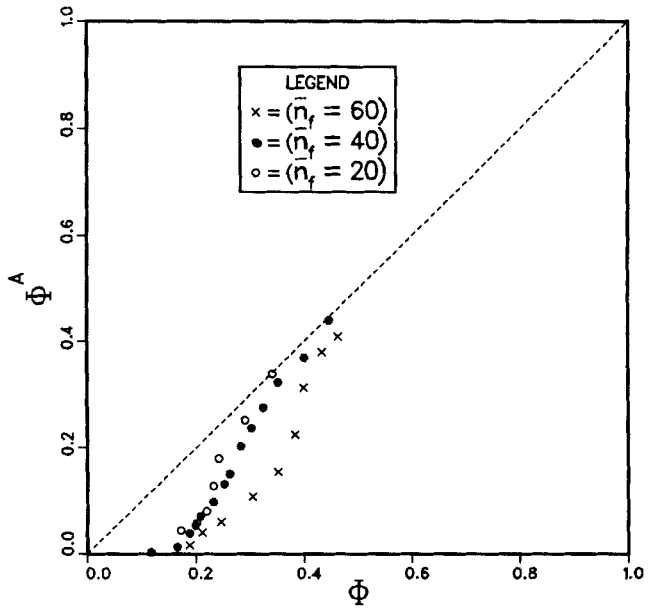

Figure 11. Accessible vs. total porosity (fully periodic boundary condition).

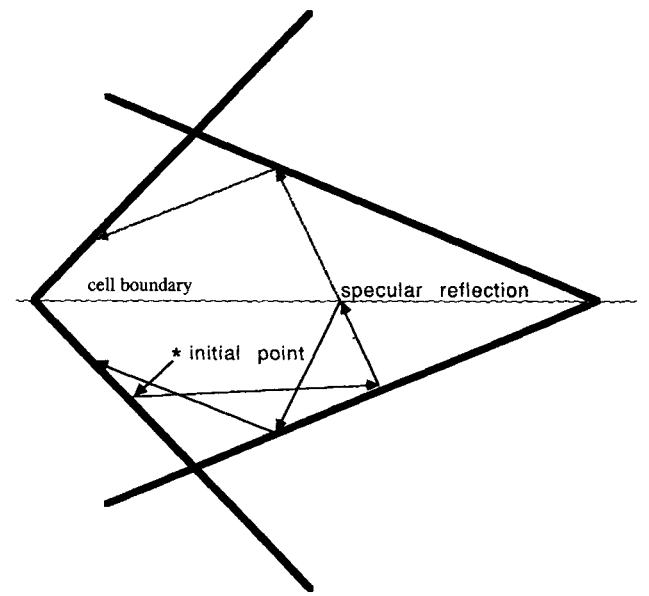

Figure 13. Pseudocluster.

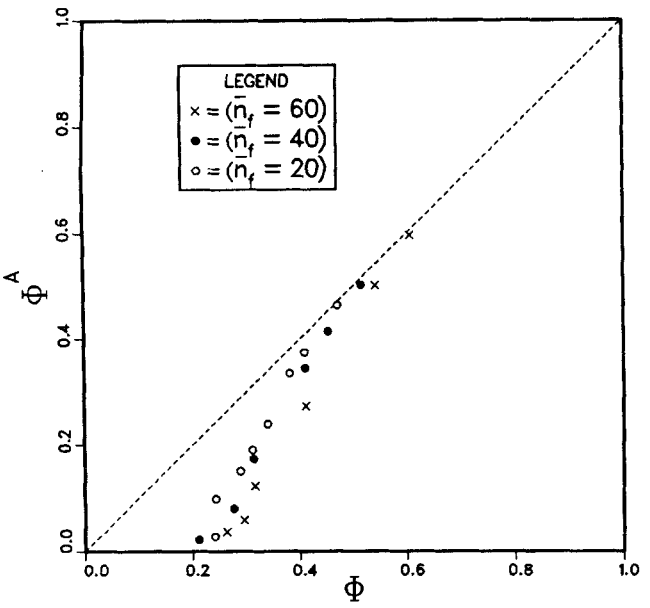

Figure 14. Accessible vs. total porosity (specular reflection B.C.).

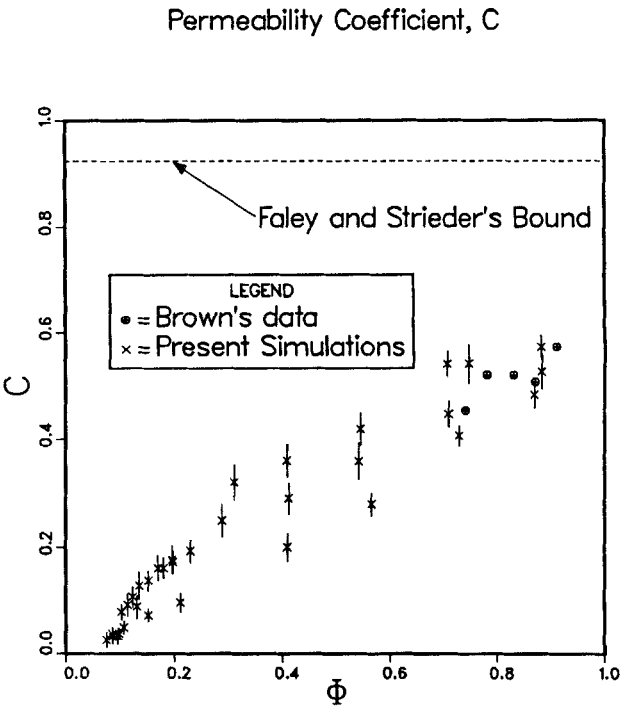

Figure 15. Permeability coefficient vs. data.

Comparisons with data

The Knudsen diffusivities obtained by simulation for fibrous media can be converted to gas permeabilities (Carman, 1956). In particular, the permeability coefficient, C, has to be related to the normalized diffusivity, ϵ (Eq. 22); equating the expressions for the effusive molecular flux in Faley and Strieder (1988) and in this paper (Eq. 12),

$$C\phi\bar{d}(2\pi\mu kT)^{-1/2} = \frac{N_0 D_K^{\text{eff}}}{RT} \tag{23}$$

Substituting Eqs. 1, 21, and 22,

$$C = \frac{4}{3}\frac{\epsilon}{\phi} \tag{24}$$

Faley and Strieder prove that $C \leq 12/13$. The values of C obtained (at three number densities) are plotted in Figure 15 along with their 95% confidence limits, and as can be seen, they all lie below the theoretical upper bound. Further comparisons can be made with experimental data obtained by Brown (Carman, 1956) for a bed of "randomized" glass fibers, which were essentially chopped fibers placed in a holder with no preferred orientation. His measurements were in the slip flow regime, just prior to the transition to Knudsen, of the quantity, δ_1/k', which appears in the slip flow term of the permeability coefficient, $\frac{1}{3}(\delta_1/k')\,\phi\bar{d}\bar{v}$. However, in the light of evidence that δ_1/k' does not vary much from its pure Knudsen equivalent (δ_0/k'),

$$C \approx \frac{4}{3}\frac{\delta_1}{k'} \tag{25}$$

The data of Brown are also plotted in Figure 15. There is excellent agreement at these high porosities.

Conclusions

In this study, we have characterized the structural and transport properties for a model of random fibrous media. An explicit MC technique used in the past was refined and used to calculate, for the first time, accessible porosities in these media. The results have direct relevance in the CVI process, where diffusivity and accessibility information at low pressures and high temperatures are needed as fibers grow with solids deposition. The MC calculated Knudsen diffusivities can be described simply when correlated with the reduced matrix density parameter, ξ. The isolated cluster formation is detrimental to the mechanical strength of the final densified composite. Attempts to minimize the extent of this internal void formation will need to take into account the dependence on n_f qualitatively demonstrated here.

Because of the low pressures commonly used in CVI, the Knudsen results are most relevant to this process. Nevertheless, it would be fundamentally interesting to extend the work to the transition and ordinary regimes. Since, in the latter regime the mean free path is (by definition) much smaller than the mean pore dimension, the techniques described here can be prohibitively expensive when applied to the computation of transport, due to the much larger number of steps a molecule must take to sufficiently "feel" the influence of the solid phase (Schwartz and Banavar, 1989).

Acknowledgment

This work was supported by a Kodak Fellowship to RRM, the Minnesota Supercomputer Institute, and the National Science Foundation (PYI).

Notation

C = permeability coefficient
$\bar{d}$ = mean pore dimension
D = diffusivity
f_T = fraction transmitted
ℓ = Knudsen free path length
k = Boltzmann constant
l_f = fiber length
L = length of simulation volume
M = molecular weight
n = number of steps
n_f = fiber number density
n_0, N_M = number of molecules
N_0 = Avogadro's number
N_T = number of trials
p = pressure
r = capillary radius
r_f = fiber radius
r_s = sphere radius
R = universal gas constant
s = specific surface area
Δs = simulation length scale
t = distance along cylinder axis
T = temperature
$\bar{v}$ = mean thermal velocity
V = volume
x, y, z = spatial coordinates
u, v, w = direction cosines

Greek letters

α, β, γ = direction angles
ϵ = normalized effective diffusivity
θ, Φ = azimuthal, zodiacal angles
λ' = measure of length of axes per volume
μ = molecular mass
ξ = reduced matrix density
ρ = sphere number density
τ = tortuosity
ϕ = porosity

Subscripts

c = cylinder
C = critical
f = fiber
Kn, K = Knudsen
max = maximum
n = normal

Superscripts

A = accessible
eff = effective
o = overlap

Literature Cited

Abbasi, M. H., J. W. Evans, and I. S. Abramson, "Diffusion of Gases in Porous Solids: Monte Carlo Simulations in the Knudsen and Ordinary Diffusion Regimes," *AIChE J.*, **29,** 617 (July, 1983).

Anderson, D. M., "Studies in the Microstructure of Microemulsion," PhD Thesis, University of Minnesota (1986).

Balberg, I., and N. Binenbaum, "Computer Study of the Percolation Threshold in a Two-Dimensional Anisotropic System of Conducting Sticks," *Physical Rev. B,* **28**(7), 3799 (1983).

Balberg, I., N. Binenbaum, and N. Wagner, "Percolation Thresholds in the Three-Dimensional Sticks System," *Physical Rev. Letters,* **52,** 17, 1465 (1984).

Burganos, V. N., and S. V. Sotirchos, "Simulation of Knudsen Diffusion in Random Networks of Parallel Pores," *Chem. Eng. Sci.*, **43,** 1685 (1988).

Caputo, A. J., and W. J. Lackey, "Fabrication of Fiber-Reinforced Ceramic Composites by Chemical Vapor Infiltration," *Ceramic Eng. and Sci. Proc.*, **5,** 654 (1984).

Carman, P. C., *Flow of Gases through Porous Media,* p. 73, Academic Press, New York (1956).

Coleman, R., "Random Paths through Convex Bodies," *J. of Appl. Probability,* **6,** 430 (1969).

Colmet, R., I. Lhermitte-Sebire, and R. Naslain, "Alumina Fiber/Alumina Matrix Composites Prepared by a Chemical Vapor Infiltration Technique," *Adv. Ceramic Mat.*, **2,** 185 (1986).

DeVera, Jr., A. L., and W. Strieder, "Upper and Lower Bounds on the Thermal Conductivity of a Random, Two-Phase Material," *J. of Physical Chemistry,* **81,** 1783 (1977).

Elam, W. T., A. R. Kerstein, and J. J. Rehr, "Critical Properties of the Void Percolation Problem for Spheres," *Physical Rev. Letters,* **52,** 1516 (1984).

Evans, J. W., M. H. Abbasi, and A. Sarin, "A Monte Carlo Simulation of the Diffusion of Gases in Porous Solids," *J. of Chem. Phys.*, **72,** 2967 (1980).

Faley, T. L., and W. Strieder, "Knudsen Flow through a Random Bed of Unidirectional Fibers," *J. of Appl. Phys.*, **62,** 4394 (1987).

———, "The Effect of Random Fiber Orientation on Knudsen Permeabilities," *J. of Chem. Phys.*, **89,** 6936 (1988).

Fanti, L. A., and E. D. Glandt, "Partitioning of Spherical Particles into Fibrous Matrices I," *J. Coll. Int. Sci.*, in press.

———, "Monte Carlo Simulation of Fluids in Curved Three-Dimensional Space," *Molecular Simulation,* **2,** 163 (1989).

Foster, M. D., "Small Angle X-Ray Scattering Investigation of Pore Structure Change in Gas-Solid Reactions," PhD Thesis, University of Minnesota, Minneapolis (1986).

Gavalas, G. R., "A Random Capillary Model with Application to Char Gasification at Chemically Controlled Rates," *AIChE J.*, **26**(4), 577 (1980).

Glandt, E. D., personal communication (1989).

Guiffant, G., and P. Flaud, "Numerical Model for the Determination of the Effective Thermal Conductivity of Composite Materials," *Int. Comm. in Heat and Mass Trans.*, **13,** 675 (1986).

Keller, J. B., "Conductivity of a Medium Containing a Dense Array of Perfectly Conducting Spheres or Cylinders or Nonconducting Cylinders," *J. of App. Phys.*, **34,** 991 (1963).

Kerner, E. H., "The Electrical Conductivity of Composite Media," *Proc. Phys. Soc.*, **69B,** 802 (1956).

Kerstein, A. R., "Equivalence of the Void Percolation Problem for Overlapping Spheres and a Network Problem," *J. of Phys. A,* **16,** 3071 (1983).

Kotlensky, W. V., "Deposition of Pyrolytic Carbon in Porous Solids," *Chemistry and Physics of Carbon,* Walker, P. L., and P. A. Thrower, eds., Marcel Dekker, New York (1973).

Landauer, R., "The Electrical Resistance of Binary Metallic Mixtures," *J. of App. Phys.*, **23,** 779 (1952).

Maxwell, J. C., *A Treatise on Electricity and Magnetism,* Vol. **1,** p. 440, Clarendon, Oxford (1881).

Marinkovic', S., and S. Dimitrijevic', "Carbon/Carbon Composites Prepared by Chemical Vapour Deposition," *Carbon,* **23,** 691 (1985).

McCullough, R. L., "Generalized Combining Rules for Predicting Transport Properties of Composite Materials," *Composites Sci. and Technol.*, **22,** 3 (1985).

Nakano, Y., and J. W. Evans, "The Relationships between Pore Classes in a Solid Computed by a Monte Carlo Technique," *Powder Technol.*, **35,** 115 (1983).

Naslain, R., H. Hannache, L. Heraud, J. Rossignol, F. Christin, and C. Bernard, "Chemical Vapor Infiltration Technique," *Proc. Euro. CVD-4,* Eindhoven, 293 (1983).

Nicholson, D., and J. H. Petropoulos, "Capillary Models for Porous Media: VII. Study of Gaseous Flow in the Transition from the Knudsen to the Counter-Diffusion Regimes," *J. Phys. D,* **10,** 2423 (1977).

Ogston, A. G., "The Spaces in a Uniform Random Suspension of Fibres," *Trans. Far. Soc.*, **54,** 1754 (1958).

Perrins, W. T., D. R. McKenzie, and R. C. McPhedran, "Transport Properties of Regular Arrays of Cylinders," *Proc. R. Soc. Lond. A,* **369,** 207 (1979).

Pfeifer, W. H., W. J. Wilson, N. M. Griesenauer, M. F. Browning, and J. M. Blocher, Jr., "Consolidation of Composite Structures by CVD," *Conf. Chemical Vapor Deposition,* 463, New York (1970).

Pierson, H. O., "Boron Carbide Composites by Chemical Vapor Deposition," *J. of Composite Mat.*, **9**, 230 (1975).
Pike, G. E., and C. H. Seager, "Percolation and Conductivity: A Computer Study: I," *Phys. Rev. B*, **10**, 1421 (1974).
Progelhof, R. C., J. L. Throne, and R. R. Ruetsch, "Methods for Predicting the Thermal Conductivity of Composite Systems: A Review," *Polym. Eng. and Sci.*, **16**, 615 (1976).
Reyes, S., "Application of Percolation Theory to Modeling of Noncatalytic Gas-Solid Reactions," PhD Thesis, University of Minnesota (1985).
Reyes, S., E. Iglesia, and K. F. Jensen, "Application of Percolation Theory Concepts to the Analysis of Gas-Solid Reactions," *Symp. on the Solid State Ionics*, **32/33**, 833 (1989).
Rossignol, J. Y., F. Langlais, and R. Naslain, "A Tentative Modelization of Titanium Carbide CVI Within the Pore Network of Two-Dimensional Carbon-Carbon Composite Preforms," *Proc. CVD-IX*, Electrochemical Society, Pennington, NJ, 596 (1984).
Sahimi, M., "On the Determination of Transport Properties of Disordered Systems," *Chem. Eng. Comm.*, **64**, 177 (1988).
Sangani, A. S., and C. Yao, "Transport Processes in Random Arrays of Cylinders: I. Thermal Conduction," *Phys. Fluids*, **31**, 2426 (1988).
Schwartz, L. M., and J. R. Banavar, "Transport Properties of Disordered Continuum Systems," *Phys. Rev. B*, **39**, 11965 (1989).
Smith, D. M., "Knudsen Diffusion in Constricted Pores: Monte Carlo Simulations," *AIChE J.*, **32**, 329 (1986).
Starr, T. L., "Model for Rapid CVI of Ceramic Composites," *Proc. of 10th Int. Conf. on CVD*, 1147 (1987).
Strieder, W. C., and S. Prager, "Knudsen Flow through a Porous Medium," *Phys. of Fluids*, **11**, 2544 (1964).
Tokunaga, T. K., "Porous Media Gas Diffusivity from a Free Path Distribution Model," *J. of Chem. Phys.*, **82**, 5298 (1985).
Torquato, S., and J. D. Beasley, "Effective Properties of Fiber-Reinforced Materials: I. Bounds on the Effective Thermal Conductivity of Dispersions of Fully Penetrable Cylinders," *Int. J. of Eng. Sci.*, **24**, 415 (1986).
Tsai, D. S., and W. Strieder, "Effective Conductivities of Random Fiber Beds," *Chem. Eng. Comm.*, **40**, 207 (1986).
Ueda, N., and M. Taya, "A New Model to Predict the Electrical Conductivity of a Misoriented Short-Fiber Composite," *Int. Conf. on Composite Materials* (ICCM-V), 1727 (1985).
Weissberg, H. L., "Effective Diffusion Coefficient in Porous Media," *J. of Appl. Phys.*, **34**, 2636 (1963).
Weissberg, H. L., and S. Prager, "Viscous Flow through Porous Media: III. Upper Bounds on the Permeability for a Simple Random Geometry," *Phys. of Fluids*, **13**, 2958 (1970).

Manuscript received May 30, 1989, and revision received Sept. 21, 1989.